

TOPICAL REVIEW

Devices for SRF material characterization

To cite this article: P Goudket *et al* 2017 *Supercond. Sci. Technol.* **30** 013001

Manuscript version: Accepted Manuscript

Accepted Manuscript is “the version of the article accepted for publication including all changes made as a result of the peer review process, and which may also include the addition to the article by IOP Publishing of a header, an article ID, a cover sheet and/or an ‘Accepted Manuscript’ watermark, but excluding any other editing, typesetting or other changes made by IOP Publishing and/or its licensors”

This Accepted Manuscript is © © 2016 IOP Publishing Ltd.

During the embargo period (the 12 month period from the publication of the Version of Record of this article), the Accepted Manuscript is fully protected by copyright and cannot be reused or reposted elsewhere.

As the Version of Record of this article is going to be / has been published on a subscription basis, this Accepted Manuscript is available for reuse under a CC BY-NC-ND 3.0 licence after the 12 month embargo period.

After the embargo period, everyone is permitted to use copy and redistribute this article for non-commercial purposes only, provided that they adhere to all the terms of the licence <https://creativecommons.org/licenses/by-nc-nd/3.0>

Although reasonable endeavours have been taken to obtain all necessary permissions from third parties to include their copyrighted content within this article, their full citation and copyright line may not be present in this Accepted Manuscript version. Before using any content from this article, please refer to the Version of Record on IOPscience once published for full citation and copyright details, as permissions will likely be required. All third party content is fully copyright protected, unless specifically stated otherwise in the figure caption in the Version of Record.

View the [article online](#) for updates and enhancements.

Devices for SRF material characterization

P. Goudket^{1,2}, T. Junginger^{3,4}, B.P. Xiao⁵

¹ASTeC, STFC Daresbury Laboratory, Warrington, Cheshire WA4 4AD, UK

²Cockcroft Institute, Warrington, Cheshire, UK

³TRIUMF Canada's National Laboratory for Particle and Nuclear Physics

⁴Helmholtz-Zentrum Berlin fuer Materialien und Energie (HZB), Germany

⁵Collider Accelerator Department, Brookhaven National Laboratory, Upton, NY, U.S.A.

E-mails: philippe.goudket@stfc.ac.uk, tobi@triumf.ca, binping@bnl.gov

The surface resistance R_s of superconducting materials can be obtained by measuring the quality factor of an elliptical cavity excited in a transverse magnetic mode (TM_{010}). The value obtained has however to be taken as averaged over the whole surface. A more convenient way to obtain R_s , especially of materials which are not yet technologically ready for cavity production, is to measure small samples instead. These can be easily manufactured at low cost, duplicated and placed in film deposition and surface analytical tools. A commonly used design for a device to measure R_s consists of a cylindrical cavity excited in a transverse electric (TE_{110}) mode with the sample under test serving as one replaceable endplate. Such a cavity has two drawbacks. For reasonably small samples the resonant frequency will be larger than frequencies of interest concerning SRF application and it requires a reference sample of known R_s . In this article we review several devices which have been designed to overcome these limitations, reaching sub - n Ω resolution in some cases. Some of these devices also comprise a parameter space in frequency and temperature which is inaccessible to standard cavity tests, making them ideal tools to test theoretical surface resistance models.

1. Introduction

1.1. The need for RF sample testing of materials for superconducting cavities

In particle accelerators superconducting RF (SRF) cavities are generally used to take advantage of the extremely low surface resistance provided by the superconductor and thereby minimize losses in the cavity walls. This is particularly interesting when high duty cycle or even continuous wave (CW) operation is required.

The material of choice for SRF cavities is niobium, as it has the highest single-element critical temperature and lower critical field H_{c1} [1] as well as good mechanical and thermal properties. Niobium cavities are generally made of bulk material, though some of the earliest cavities were Nb-coated copper cavities used for the LEP [2] taking advantage of the higher thermal conductivity of copper. This approach also has the advantage of the lower price of copper compared to niobium. Niobium-on-copper cavities have a lower surface resistance at 4.2 K (at low gradient levels) and do not require shielding from the Earth's magnetic field. Currently this approach is used for cavities in the LHC and HIE-Isolde at CERN and ALPI at INFN Legnaro. Current performance levels of niobium-coated copper structures are inferior to those of bulk niobium technology, as their surface resistance increases strongly with field. New deposition techniques are being developed to overcome current limitations. Some of them are not on a technological readiness level

2

for deposition on a cavity and therefore require testing of small samples to probe their RF performance and streamline optimization of the coating process.

Theoretically the maximal field achievable under RF is defined by the superheating field H_{sh} of the cavity material. For the case of niobium, a type-II superconductor, this is about 240 mT (at 0 K), which corresponds to an accelerating gradient of 57 MV/m [3] for the widely used TESLA shaped cavity. In practice after years of development and optimization of cavity shapes, manufacture and processing techniques accelerating gradients in excess of 50 MV/m [4] and Q-values close to the theoretical limit are achieved in single-cell Nb cavities at frequencies of 1.3 GHz. Bulk niobium technology is thus approaching its fundamental limitations. Optimization of the cavity shape can push the maximum Q-value and accelerating gradient by some percent but to achieve a performance significantly exceeding the state of the art one has to change to materials other than bulk niobium. Therefore there is an active field of research into new materials potentially displaying higher performance than niobium, such as NbN, NbTiN, MgB₂ and Nb₃Sn [5]. Of these materials only Nb₃Sn has been successfully deposited on an SRF cavity and shown to have a performance exceeding bulk niobium at least at 4.2 K for a moderate accelerating gradient [6]. To assess the RF performance of other new materials and optimize coating procedures the community currently has to rely on sample tests.

As mentioned above best performance of materials other than niobium has been achieved with Nb₃Sn. Results however suggest that this material is currently limited by vortex penetration at fields at defects far below its superheating field [7]. Strong dissipation from vortex penetration could possibly be avoided by depositing nanometer-thin multilayers of superconductors and insulators on a niobium cavity, as suggested in 2006 by A. Gurevich [8]. So far only small samples have been produced since this complex technology is not yet ready for depositing films on full scale cavities. Therefore, this is another process whose optimization depends on the testing of small samples.

The operational limitations of elliptical SRF bulk niobium cavities have been pushed back over the many years of research since their first use. We are now approaching the fundamental limits of this material. However, neither cavities of different shape, such as quarter wave resonators, nor cavities of different materials such as Nb₃Sn are performing close to their fundamental limits. While the ideal approach to test new materials for SRF applications is to produce cavities as used in the particle accelerators, this approach is costly and some materials are not yet developed enough and require testing of small samples.

This article focuses on devices which allow measuring the surface resistance of samples. Before performing these tests samples can be characterized by several DC methods. These include RRR measurements [9] which give information on the sample purity and electron mean free path, and AC susceptibility measurements [10] which are typically performed at 100 Hz -10 kHz and can give information on flux dynamics. DC SQUID magnetic susceptibility measurements [11] allow one to gain information on the magnetization curve of the sample. Attempts have been made to extract the H_{c1} and H_{c2} from this curve, but this requires complex sample alignment and interpretation of the results is still controversial. Also possible are field penetration measurements, which is a technique dating from the 1930s but only recently used for thin film measurements [12]. Several other material and surface analytic techniques have been applied to SRF cavity materials. An overview can be found in reference [13]. All these DC methods can be useful to characterize the film quality and can guide coating parameter optimization. They fail however to predict the RF performance of the samples. It is thus required to test these samples under RF exposure to relate the surface properties to the RF performance.

While this article focuses on devices which allow measuring the surface resistance of samples, other methods to characterize RF losses exist and are being briefly reviewed in the following section.

1.2 Other methods to measure losses of superconductors under RF

The sample test cavities which will be reviewed in the following chapter all allow the measurement of the surface resistance of an attached sample. Other options to explore the loss mechanisms of superconductors under RF exposure are beyond the scope of this article. However in this section some alternative approaches will be briefly mentioned. The most straightforward option is to use single-cell cavities and measure their quality factor. The surface resistance derived from this measurement has then to be taken as averaged over the whole surface area. To gain information about the distribution of the losses on the sample surface several temperature sensors can be placed on the cavity's outer surface. This widely used technique is called temperature mapping or simply T-mapping [3]. In order to gain direct information about the temperature distribution on the inner cavity surface JLab has developed a laser beam scanning apparatus [14]. This laser beam not only allows measurement of the surface temperature but can also be used to move vortex hot spots. Pushing them to lower field regions can significantly decrease the overall losses [15].

Most single cell cavity tests have been performed on 1.3 or 1.5 GHz cavities, which are large compared to typical sample sizes of the devices focused on in this article. INFN Legnaro has developed an infrastructure to test significantly smaller 6 GHz cavities allowing for quick turnarounds, since these cavities can be directly inserted into a liquid helium dewar [16]. A helium transfer from a dewar to a test cryostat is thus not required. Evidence for thermal boundary resistance effects on the surface resistance of niobium cavities was found [17].

Most surface resistance studies have been performed on elliptical cavities. An open question in SRF is why cavities of different geometries like quarter or half wave cavities generally exhibit a stronger decrease of the quality factor Q_0 with applied field strength. TRIUMF is currently developing coaxial resonators which can be heat treated in an induction furnace to explore this in detail [18].

All devices presented in this article are designed to measure the surface resistance of samples with diameters of typically a few cm. University of Maryland scientists have developed a system to measure third harmonics nonlinearities of superconductors in the sub-micrometer scale using a magnetic write head. Niobium and MgB_2 have been investigated. The nonlinear response was found to be localized in niobium and uniform in MgB_2 [19].

2. Measurement techniques

In order to measure the surface impedance of a sample surface, it is necessary to make the sample a part of a resonant structure. Such a sample could be a rod [20, 21], a flat disc [20, 22-34] or just a small piece [20, 35, 36] inserted into the cavity inner surface. The cavity is then excited in a particular mode with the resonant frequency and Q_0 easily measurable, allowing one to calculate the surface impedance in a straightforward way [20, 22, 23, 25-30, 37, 38] based on average losses and differential measurements with calibrated samples. Another way to measure the surface impedance with significantly higher resolution is to use a power compensation technique that combines calorimetric measurements with RF measurements [24, 31-36].

2.1. Choice of cavity geometry

Cylindrically symmetric cavities operating in a TE_{0xx} mode are commonly chosen as the resonant circuits [20, 21, 23, 25, 28-34, 37, 38]. In such a cavity with these modes the electric field lines are simple self-closing rings around the resonator axis and electric field lines vanish on cavity walls as well as on the sample, if positioned at the lateral end of the cavity. Moreover, in the ideal geometry, no RF current crosses the joint between the sample and the cavity and, with no electric fields normal to the cavity surface, electronic problems such as multipacting and heating due to dark current may be avoided.

For simple cavity geometries, these TE_{0xx} cavities can only be used to measure large-sized samples while maintaining suitably low resonance frequencies.

4

Other attempts with more complicated geometries, including the “triaxial” cavity [24], “quadrupole mode resonator” [35, 36], “mushroom cavity” [26, 27] and sapphire loaded Surface Impedance Characterization (SIC) cavity [31-34] have been made, trying to overcome the limitation of simple TE mode cavities.

2.2. Choice of measuring technique

A simple way to measure the surface resistance is to measure the quality factor Q_0 change with a reference sample and the sample to be measured, so called end-plate replacement technique, which is used since more than 40 years [39]. It requires a reference sample. The reference sample is usually surface treated using the same way of the cavity, so that the surface resistance of the cavity and the sample are the same. Using a copper cavity as an example, we assume the quality factor of the cavity with reference sample Q_1 at 2×10^5 , geometry factor G at 300, filling factor of the sample η (the loss on the reference sample versus the total loss) at 40%, and the sample's surface resistance R_s is much smaller than the surface resistance of copper. Then Q_2 , the quality factor of the cavity with sample to be measured, should be 5×10^5 . R_s can be calculated using

$$R_s = \frac{G}{\eta} \left(\frac{1}{Q_2} - \frac{1}{Q_1} \right) + \frac{G}{Q_1} \quad (1)$$

Typically, the quality factor measurement error will be about 5%, from equation (2)

$$\Delta R_s = \sqrt{\left(\frac{G \Delta Q_2}{\eta Q_2^2} \right)^2 + \left[G \left(1 - \frac{1}{\eta} \right) \frac{\Delta Q_1}{Q_1^2} \right]^2} \quad (2)$$

one can get that ΔR_s should be 0.14 m Ω . In this case quality factor measurement with a copper cavity is not preferred for SRF samples. In a case where a niobium cavity with a Q_1 at 2×10^9 was used, ΔR_s would be improved to 14 n Ω . Despite its lower resolution compared to the other techniques introduced below, this approach is still used, since it allows for designing simple systems and performing quick tests.

Another way to measure the surface resistance with a significantly higher resolution is a power compensation technique, which allows the derivation of the surface resistance from a DC measurement. In a calorimetric system the sample and the host cavity are thermally decoupled. A DC heater (resistor) and at least one temperature sensor is attached to the back side of the sample. This allows for independent control of the sample temperature.

A calorimetric measurement consists of two steps, see Figure 1:

1. The temperature of interest is set by applying a current to the resistor on the back side of the sample. The power dissipated P_{DC1} is derived from measuring the voltage across the resistor.

2. The RF is switched on and the current applied to the resistor is lowered to keep the sample temperature and the total power dissipated constant.

The RF power dissipated in the sample, P_{RF} , is the difference between the DC power applied without RF, P_{DC1} , and the DC power applied with RF, P_{DC2} . P_{RF} is directly related to the surface resistance of the sample R_s and the magnetic field on the sample surface B ,

$$P_{RF} = P_{DC1} - P_{DC2} = \frac{1}{2\mu_0^2} \int_{Sample} R_s(B) |\vec{B}|^2 dS \quad (3)$$

Assuming R_s to be constant over the sample surface area and independent of B , the above equation simplifies to:

$$P_{RF} = P_{DC1} - P_{DC2} = \frac{R_s}{2\mu_0^2} \int_{Sample} |\vec{B}|^2 dS \quad (4)$$

which can be rearranged to yield an expression for the surface resistance:

$$R_s = \frac{2\mu_0^2 (P_{DC1} - P_{DC2})}{\int_{Sample} |\vec{B}|^2 dS} \quad (5)$$

An electromagnetic simulation and an RF calibration is needed to relate $|B|^2 dS$ to the transmitted power measured in the experiment. Details are described in references [33, 40].

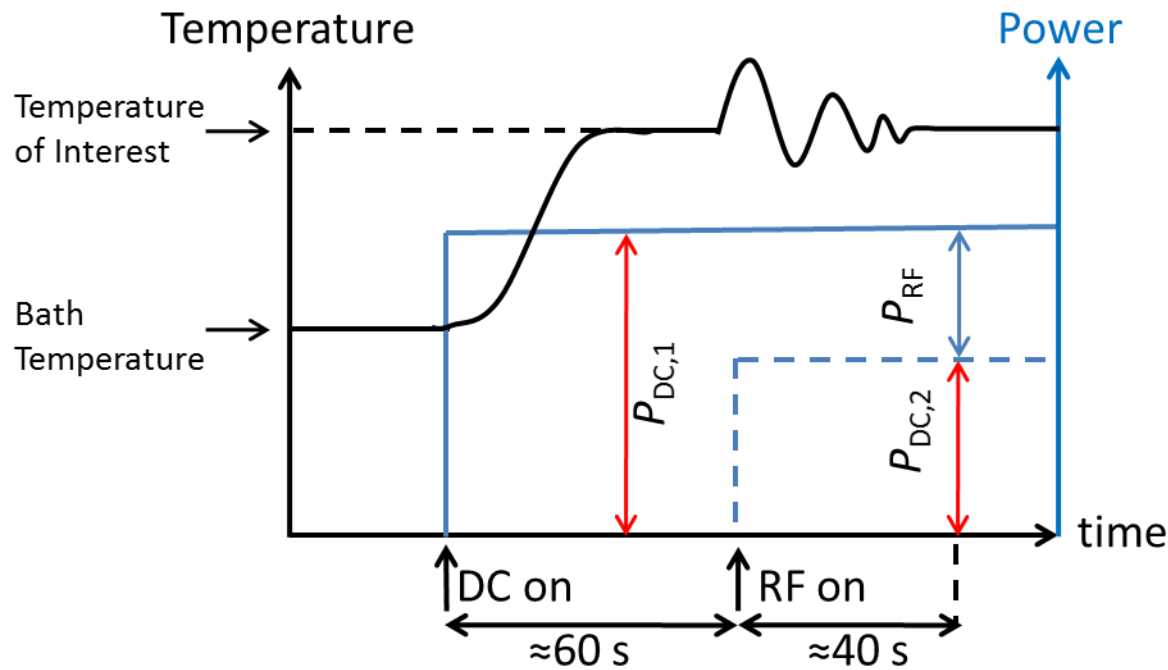


Figure 1: In a calorimetric system the surface resistance of a superconducting sample is derived from a DC measurement [40].

The calorimetric measurement gives a high resolution on the surface resistance measurement. The DC power is measured using a four-probe technique, and a high-precision current source and voltmeter. Temperature measurements give a resolution better than 5 mK. The magnetic field is calculated from RF power measurements and decay time measurement, with an accuracy better than 5%. The slow variation of helium bath pressure can be ignored since the data is taken within a few minutes. The ripple of the helium bath pressure, normally better than 100 μ bar, will give a 1 mK temperature fluctuation at 2 K bath temperature, which can already be better than the resolution of the thermal sensors. Finally the resolution of a calorimetric system will be limited by the minimal detectable heating and therefore depend on the resolution of the voltmeter and temperature readout. Thus the resolution can be obtained by differentiating equation (5) with respect to P_{DC2} yielding:

$$|\Delta R_s| = \frac{2\mu_0^2 \Delta P_{DC2}}{\int_{Sample} |\vec{B}|^2 dS} \quad (6)$$

This equation directly shows why these systems have a much higher resolution for R_s for higher fields. The resolution of ΔR_s can be in sub- n Ω range since it is mainly limited by the DC power measurement.

The above two methods are not sufficient for investigating localized effects that will cause non-uniform temperature distribution on the sample. Temperature mapping system could be a supplemental system to investigate the non-uniform RF loss mechanism on the sample. In these systems, diodes, carbon Allen-Bradley thermal sensors, or CernoxTM thermal sensors will be mounted on the back of the sample (opposite to the surface that is exposed to the RF) near the high magnetic field region. A 4-wire setup is used to accurately measure the temperature with sub mK to 10 mK resolution. Apiezon[®] N grease is usually applied on top of each thermal sensor to ensure good thermal contact between cavity surface and sensor, together with the pressure provided by a spring loaded pin that will get compressed during the test.

6

3. An overview of devices

The early activities of developing devices for surface impedance measurement of SRF sample material can be traced back to the early 1970s. Bruynseraede et al. used a cylindrical TE_{011} cavity to measure the surface resistance of lead, indium and an indium-lead alloy by the sample replacement technique [39]. Different cavity shapes and measurement techniques were investigated in the 1980s. For example, Delayen et al. designed apparatuses to measure samples with different geometries, like rods, small samples and flat rounded samples [20]; Kneisel et al. designed a cylindrical TE_{011} Nb cavity to measure flat rounded samples [25], with a temperature mapping system on the bottom of the sample to resolve the spatial resistance difference; Klein et al. used a cylindrical TE_{011} Cu cavity to measure the surface resistance of YBCO [28] between 4 K and room temperature; Liang et al. designed a “triaxial” cavity to measure 1 inch diameter samples at 1.5 GHz below 25 mT [24]. In the new century these activities exploded all around the world, with a variety of RF designs to focus the magnetic field on the sample and trying to maintain low resonant frequencies while keeping the sample size small [26, 27, 30, 31, 33, 35, 40-44]. These activities become critical with the rapid developments on pushing the performance of bulk Nb cavity to its theoretical limitations [4, 45-47], as well as the theoretical and experimental breakthrough of thin films [6-8]. In this section we focus on devices which are currently used or under development. These are the SIC system from JLab, the quadrupole resonators from CERN and HZB, the mushroom cavities from three different labs, the cylindrical cavity from CEA Saclay and IPN Orsay, and the choked resonator under development at STFC Daresbury.

3.1. SIC

The SIC system is based on a cylindrical polycrystalline niobium cavity with 2 cm inner diameter, shown in Figure 2. A HEMEX[®] sapphire rod from Crystal Systems is inserted into the cavity to lower the resonant frequency from around 20 GHz (without sapphire) to 7.4 GHz in the TE_{011} mode. An adjustable loop input coupler is located above the cavity, and its external quality factor can be varied from 10^6 to 10^{10} for this mode. The sapphire is tightly held from the top, and its bottom surface is set to be coplanar with the bottom of the cavity. The sample is located at the open end of the cavity and is thermally isolated from the bottom plane of the cavity cylinder and sapphire, being separated from them by a 0.02 cm gap. Two RF choke joints with a 1 cm depth are used at the bottom of the cavity to minimize the RF power leakage. This system provides well-controlled RF fields within the central 0.8 cm^2 area of samples with 5 cm in diameter. Cylindrically symmetric cavity operating in a TE_{011} mode is chosen as the resonant circuit for the SIC RF system. In such a cavity with this mode, the electric field lines are simple self-closing rings around the resonator axis and electric field lines vanish on cavity walls as well as on the sample, if positioned at the lateral end of the cavity. Moreover, in the ideal geometry, no RF current crosses the joint between the sample and the cavity and, with no surface-normal electric fields, electronic problems such as multipacting and heating due to dark current may be avoided. Compared to other designs, the SIC system inherits the merits of TE structure cavities and offers a good solution to the size issue while keeping the resonant frequency relatively low. And the unique design of the SIC system guarantees controlled RF field within the center of the sample, which simplifies the sample and sample holder structure and ensures the success of the RF-calorimetric combination measurement. The sample edges and the joint between sample and sample holder are shielded from high RF fields, therefore anomalous heating from vortex entry at edges is avoided. The sample mounting system is designed to be able to quickly swap the sample and to adopt a variety of samples with different substrates. The SIC uses the high precision calorimetric measurement technique. In a typical measurement with more than 5 mT applied magnetic flux density, the resolution of R_s will be 1.1 n Ω at 2 K and 6.6 n Ω at 9

7

K. However the SIC system works at a frequency much higher than cavity operation frequency, which is normally at 1.3 or 1.5 GHz, and the highest achieved magnetic field is at 14 mT.

The SIC system is used to measure the R_s of a variety of samples. Besides bulk Nb and thin film Nb samples [32, 33, 48, 49], this system is also used to measure the alternative materials like MgB_2 [50], Nb_3Sn [51], NbN [52] and $NbTiN$ [53], as well as different multilayer thin films: $NbTiN-AlN-Nb$, $NbTiN-AlN-Nb-Al_2O_3$, $NbN-MgO-Nb$, $MgB_2-MgO-Nb-MgO$ [52, 53], and $Nb_3Sn-Al_2O_3-Nb$ [54]. At 7.5 GHz, the single crystal MgB_2 films on 5 cm diameter sapphire disks fabricated by a hybrid physical chemical vapor deposition (HPCVD) revealed a $9 \pm 2 \mu\Omega$ surface resistance at 2.2 K, and exhibited a lower surface resistance than Nb at temperatures above 4 K [50].

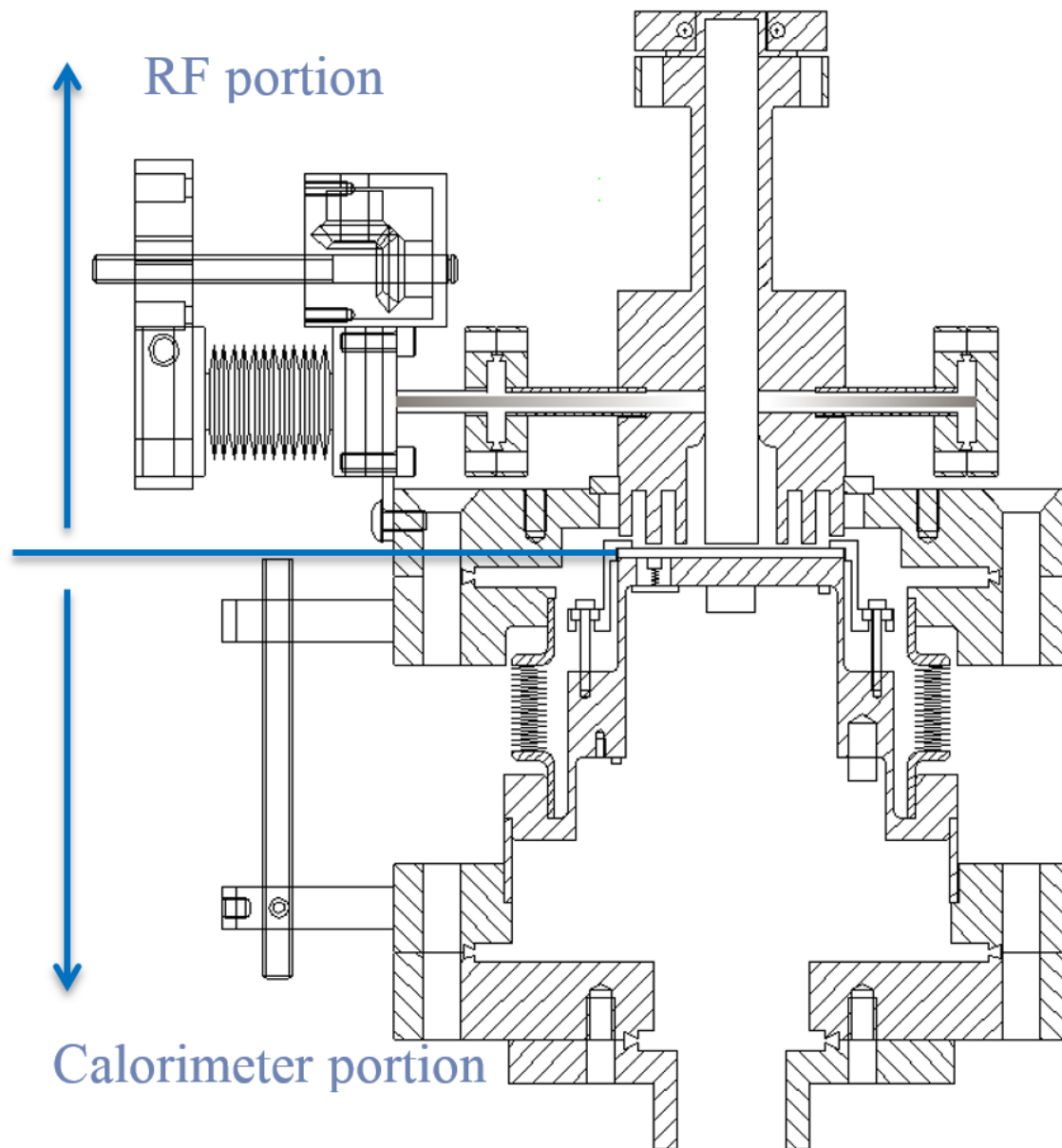


Figure 2: SIC system overview, the top part is the RF portion and the bottom part is the calorimeter portion, with two parts joined by the 5 cm diameter sample. The RF portion includes a sapphire-loaded cylindrical

8

cavity with choke joints, one fixed pickup coupler and one tunable fundamental power coupler. The calorimeter portion includes a sample holder with sensors and heaters, and a thermal path to the helium bath. [33]

3.2. Quadrupole resonator

3.2.1. CERN Design

The quadrupole resonator shown in Figure is a four-wire transmission line half-wave resonator designed and built in 1997 for excitation in a TE_{210} -like mode at 400 MHz [35]. The magnetic field is at its maximum on the top plate where the resonator rods are attached to the host cavity on the crooked rods illuminating the sample surface at the bottom. The geometry also allows for excitation at multiple integers of 400 MHz (TE_{211} , TE_{212} -like...). In the case of the 800 MHz mode there is one additional peak along the rod, while in the case of the 1200 MHz mode there are two additional peaks along the rod. It has been commissioned for the frequencies of 400, 800 and 1200 MHz [55].

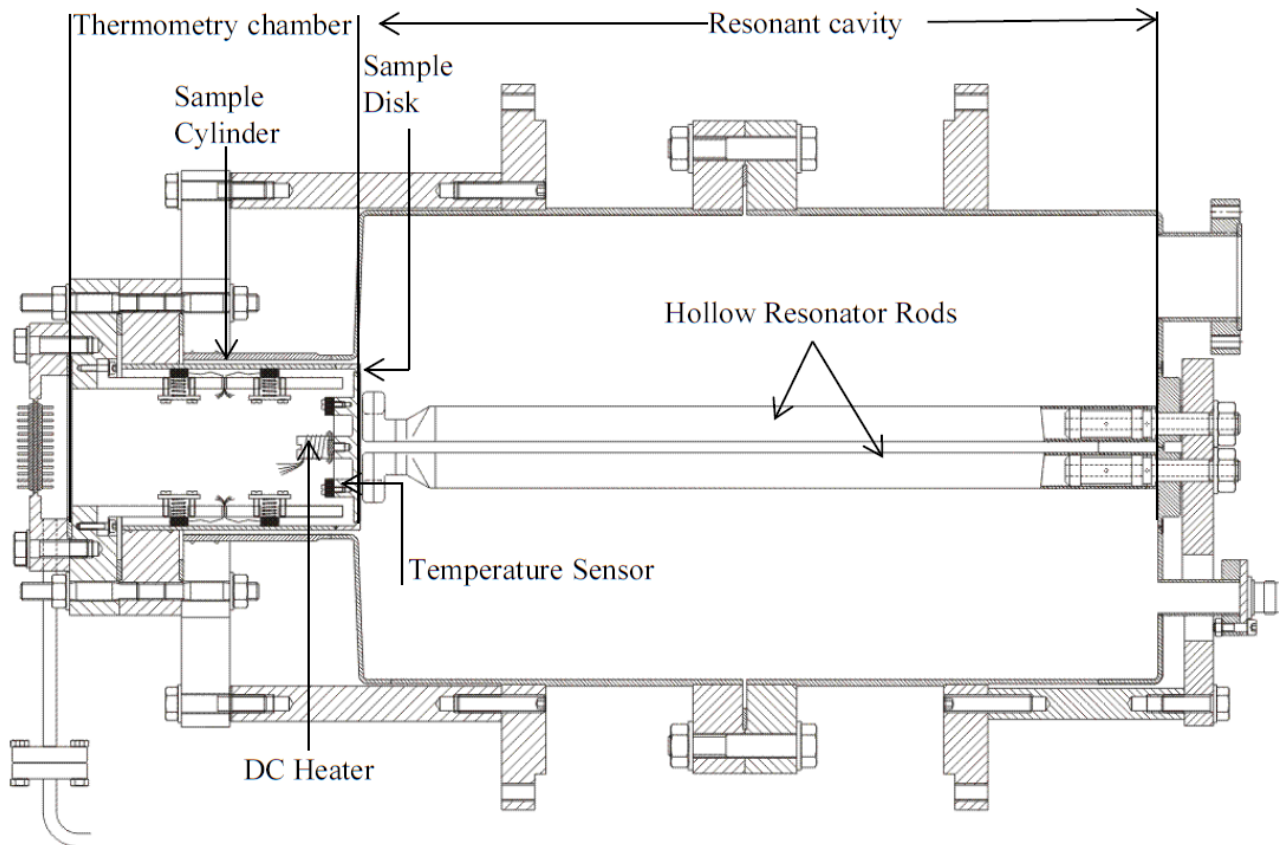


Figure 3: Quadrupole resonator: The sample disk is electron beam welded to the sample cylinder, which forms a coaxial structure with the host cavity. Inside of this narrow gap, the RF fields are exponentially decaying limiting the losses at the flange where the sample cylinder is mounted onto the host cavity. [35, 55]

The quadrupole resonator consists of two 2 mm thick niobium cans for convenient handling and cleaning of the device, as shown in Figure . These cans are flanged to each other in the middle of the resonator, where the screening current on the cavity surface vanishes for the modes at 400 and 1200 MHz. For the 800

1
2
3
4 285 MHz mode the screening current has a maximum at this position. However, since the field is strongly con-
5 286 centrated around the rods in the middle of the resonator, excitation and measurements at 800 MHz are not
6 287 perturbed by losses at this flange. The quadrupole resonator is equipped with two identical strongly over-
7 288 coupled antennas. One serves as the input, the other as the output. Due to this configuration almost the
8 289 whole power transmitted to the cavity is coupled out and only about 1% is dissipated in the cavity walls
9 290 and on the sample surface. The system acts like a narrowband filter with minor losses.

10 291 The cover plate of a cylinder attached to the cavity in a coaxial structure serves as the sample, see
11 292 Figure 3. This design yields exponentially decaying RF fields between the outer wall of the sample cylinder
12 293 and the host cavity. Therefore, the power dissipated inside this 1 mm gap and at the end flange and joint of
13 294 the sample cylinder is negligible. A DC heater and several temperature sensors are attached to the back side
14 295 of the sample, which is thermally decoupled from the host cavity. As in the SIC the surface resistance of
15 296 the sample is measured by the calorimetric method explained in Section 2. The resolution in case of a
16 297 niobium sample for an applied field of 5 mT at 400 MHz is 0.44 n Ω at 2 K and 2.2 n Ω at 8 K limited by the
17 298 resolution of the temperature controller which is 0.1 mK. For higher magnetic field the resolution is better,
18 299 while for materials of higher thermal conductivity, in particular niobium films on copper substrate, it is
19 300 worse [40]. The maximum field obtained with the Quadrupole resonator is 70 mT at 400 MHz limited by a
20 301 quench of the cavity. This limit is reached independent of duty cycle suggesting that it is not a thermal
21 302 limitation.

22 303 One major difference between the Quadrupole Resonator and most similar devices is that the sample is
23 304 illuminated by RF magnetic and electric fields simultaneously like the surface in accelerating cavities.
24 305 While the magnetic field configuration is almost identical for the three used quadrupole modes, the ratio
25 306 between magnetic and electric field is different for each mode. It scales quadratically with frequency. This
26 307 follows directly from the law of induction for the quadrupole resonator geometry. This feature can be used
27 308 to distinguish between electric and magnetic losses. An upgrade of the system with a coil around the sample
28 309 cylinder enables testing the influence of flux trapping and cooldown speed on the surface resistance [40].

29 310 Measurements on a bulk niobium sample at three frequencies and several temperatures have shown that
30 311 the losses from thermally activated quasiparticles (from the so called BCS surface resistance) factorize in a
31 312 field and a frequency dependent part [40]. A comparison of a niobium film sample with a bulk niobium
32 313 sample of same residual resistance ratio (RRR) was performed. Comparing these results to the microstruc-
33 314 ture of Nb films suggest that a low crystal defect density and an excellent adhesion of the film on its sub-
34 315 strate are key aspects for niobium film cavities with a performance equal to bulk niobium technology [56].

35 316 36 317 37 318 3.2.2. HZB Quadrupole Resonator

38 319 Based on the CERN design a modified version of the Quadrupole Resonator has been developed [57]. The
39 320 design frequency has been shifted to multiple integers of 433 MHz in order to use existing RF equipment
40 321 optimized for 1.3 GHz. A number of relevant figures of merit have been improved to provide a higher
41 322 resolution, a lower peak electric field and less sensitivity to microphonics [57]. The new device has been
42 323 successfully commissioned and a peak magnetic field on the sample surface of 120 mT has been achieved
43 324 [43], which is almost twice as high as what has been possible using the CERN version. One drawback of
44 325 the Quadrupole Resonator is that the sample disk has to be electron beam welded to the sample cylinder.
45 326 Most thin film deposition devices are not suitable to accommodate the whole sample cylinder. Therefore it
46 327 is necessary to coat the sample disk first and weld it afterwards to the cylinder as has been done in [56].
47 328 This procedure carries the risk of a contamination after deposition. An alternative calorimetry chamber was
48 329 developed, providing samples of 12 mm height which are easily exchangeable. The parts are connected by
49
50
51
52
53
54
55
56
57
58
59
60

10

1
2
3
4 330 screwing connections and sealed using indium wire gaskets. Flexibility in mounting height and exchange-
5 331 ability of samples between the resonators at HZB and CERN are achieved by adapting individual bottom
6 332 flanges [58].
7 333

8 334 3.3. Mushroom cavities 9 335

10 336 In a cylindrically symmetric cavity operating in a TE_{0xx} mode with a sample placed at one open end, a
11 337 higher ratio of diameter/length is preferred to confine magnetic field on the sample. However, this setup
12 338 will also produce high magnetic field at the end opposite to the sample. By deforming the shape of this end,
13 339 the highest magnetic field could be shifted and averaged. The SLAC mushroom cavity [26, 27] uses TE_{013}
14 340 like mode at 11.4 GHz with 2 inch diameter sample. Three TE_{011} modes have been stacked together and the
15 341 top plate has been reshaped to a mushroom structure, so that the magnetic field could be averaged on a
16 342 larger surface area. The peak magnetic field on the sample is 2.5 times of the peak magnetic field on the
17 343 cavity wall. The SLAC mushroom cavity is constructed out of copper so that pulsed RF power could be
18 344 conducted into the cavity and the loaded Q will not degrade that much until the sample reaches its critical
19 345 field. The Q of this Cu cavity with a Cu sample is measured to be 50,000 at room temperature and 224,000
20 346 at 4K. The Q of this Cu cavity with a superconducting sample is measured to be 342,000. The drawback of
21 347 using a copper cavity is that the Q of the whole setup is mainly determined by the copper cavity, and is less
22 348 sensitive to the contribution from the superconducting sample. The precision of the surface resistance meas-
23 349 urement is estimated to be up to 0.1 m Ω . The maximum magnetic field that can be reached in the current
24 350 system is up to 300-400 mT, it is excellent for precise measurement of the quenching magnetic field of the
25 351 superconducting samples. Recently a Cu mushroom cavity with Nb coating was fabricated and commis-
26 352 sioned at SLAC. The Q of this Nb cavity, with a single crystal bulk Nb reference sample that is assumed to
27 353 have the same surface resistance as the cavity, is around 2×10^7 , with helium bath temperature at 4 K. The
28 354 surface resistance of the reference sample is estimated to be 65 $\mu\Omega$. [59]
29 355

30 356 The Cornell mushroom cavity [41, 44], with cavity geometry similar to the SLAC version, is a niobium
31 357 cavity that provides higher measurement resolution. The peak magnetic field on the sample is 1.57 times
32 358 greater than the peak magnetic field on the cavity wall for the TE_{013} like mode at 6.16 GHz, and 1.24 times
33 359 greater for the TE_{012} like mode at 4.78 GHz, with sample diameter of 4 inches. A third generation of this
34 360 cavity resonates at 3.9 GHz and reaches a peak field over 100 mT on the sample surface and an unloaded
35 361 cavity Q_0 over 10^{10} . Recently this cavity has been used to measure the surface resistance of samples pro-
36 362 duced by High Power Impulse Magnetron Scattering (HiPIMS) [60].
37 363

38 364 Another mushroom cavity is designed at TAMU [42, 61]. The sample size of this cavity is 7 inch in
39 365 diameter. Sapphire is inserted into the mushroom cavity to reduce the resonance frequency of the TE_{01} mode
40 366 to 2.2 GHz. In this model, the maximum surface magnetic field in the cavity is 9.02 times higher than the
41 367 field anywhere else in the cavity. This cavity is shown in Figure below [42].
42
43
44
45
46
47
48
49
50
51
52
53
54
55
56
57
58
59
60

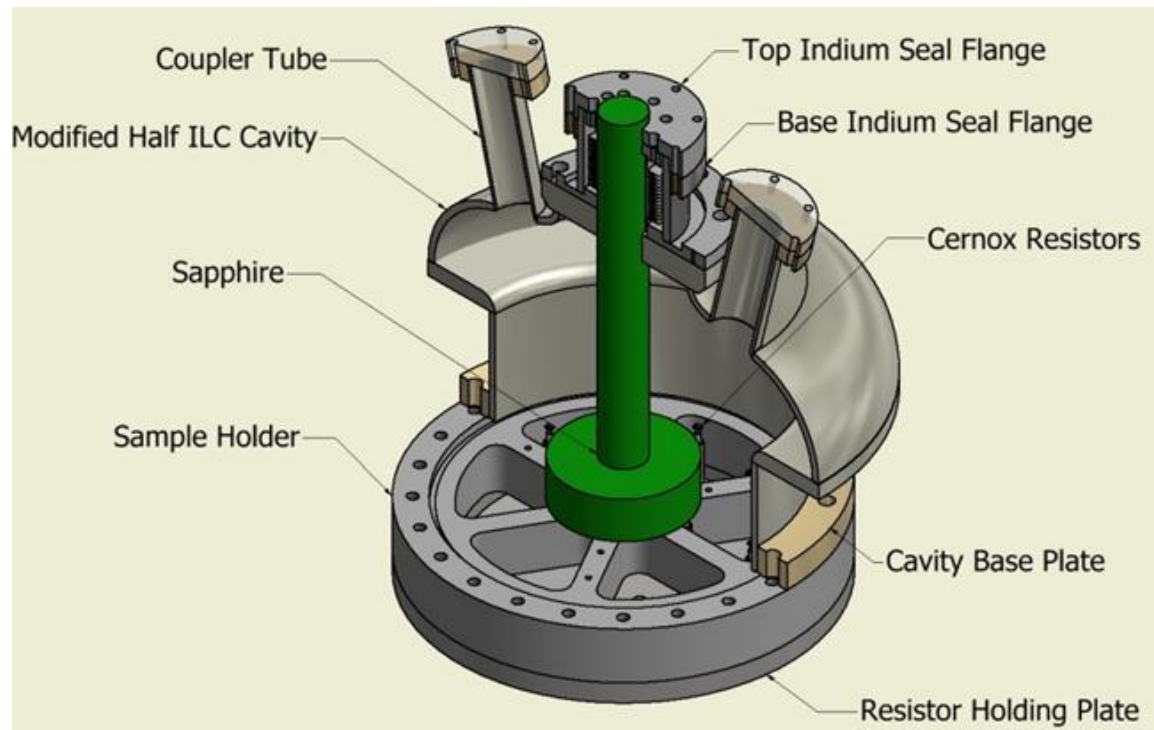


Figure 4: The Wafer Test Cavity. In the center, the sapphire is hung slightly above the surface of the sample located at the bottom. The sample (not shown in this figure) is held by a mating bottom flange containing an array of CernoxTM resistor thermometry. The sapphire extends beyond the cavity for cooling and as a means of mechanical stabilization. Two side ports are located on upper part of the cavity to provide power, insert diagnostic tools such as a probe antenna, and vacuum port. [42]

The SLAC mushroom cavity has been used to measure the surface resistance and the RF quench field of Nb and MgB₂[27]. The Cornell mushroom cavity, and its alternative, sample host cavity, is used to measure bulk Nb and thin film Nb up to 106 mT, and it is planned to be used in investigating thin-film materials such as NbN on MgO, thin-film Nb, Nb on Cu on Nb, and MgB₂[41, 44, 60].

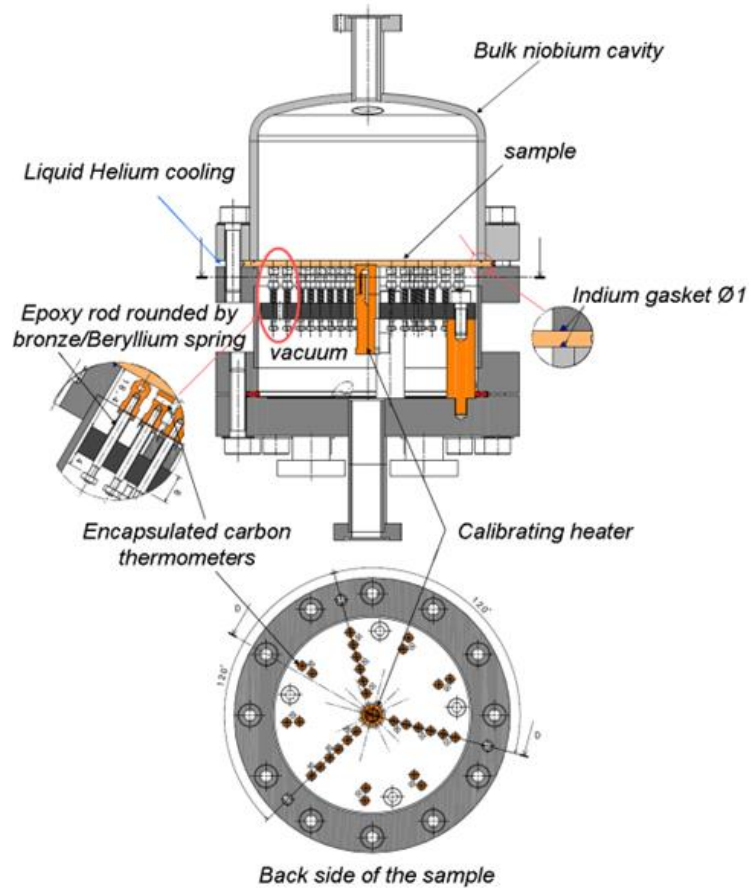
3.4. Orsay cavity

A cylindrical TE₀₁₁/TE₀₁₂ cavity enabling measurements at 4 and 5.6GHz has been developed in collaboration between CEA Saclay and IPN Orsay [22, 62] to test the surface resistance of superconducting Nb and NbTiN thin films sputtered on removable copper disks. The goal was to develop a system with improved accuracy, especially at 4 K, compared to a cylindrical niobium cavity, which used the end-plate replacement technique, relying on a reference sample. It gave a resolution of about ± 1000 n Ω at 4K. The developed calorimetric system consists of a cylindrical cavity and a thermometric part. The thermometric part is located in a vacuum insulation jacket, where a dismantable assembly with a static heater and 24 thermometers is installed, see Figure [62].

The cavity has been used for systematic studies of the surface resistance of sputtered niobium on copper samples. Substrates of different roughness have been investigated. A correlation between surface roughness and surface resistance could be made, see reference [22]. The residual resistance of the thin film samples was found to scale linear with frequency [22]. More recently a slightly modified cavity based on the same geometry has been developed for further thin film studies [30]. This cavity has been used to measure the

12

1
2
3 surface resistance of a sample comprised of nanometer thin alternating superconducting and insulating lay-
4 393 ers for the first time [63]. For a low surface magnetic field of 1 mT and temperatures above 3 K the surface
5 394 resistance of the multilayered sample was found to be significantly lower than for a niobium reference
6 395 sample.
7 396



36 397
37 398 Figure 5: Set-up of the TE_{011}/TE_{012} cavity. Reproduced with the permission of G. Martinet.

38 399
39 400
40 401
41
42
43
44
45
46
47
48
49
50
51
52
53
54
55
56
57
58
59
60

3.5. Choked resonator

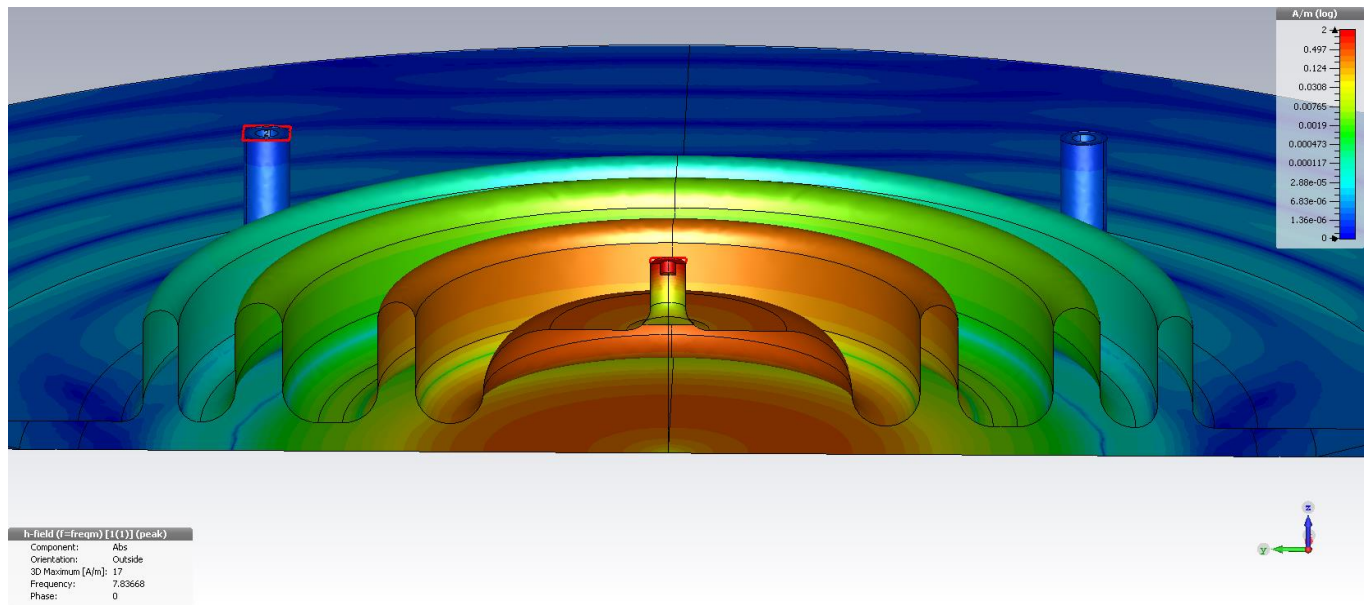


Figure 6: Simulated magnetic field intensity distribution on the cavity (top) and sample (bottom) surfaces.

A system currently in development is the Choked Resonator. It is designed to allow fast sample changes while not compromising performance and accuracy. The design called for a simple system able to measure flat sample surfaces without requiring complex assembly procedures or having to worry about the quality of the join between sample and cavity.

It operates in a TM_{010} -like mode (see Figure 6) and consists of two parts:

- A bulk niobium resonator, surrounded by RF chokes optimized to minimize the leakage field. The RF input coupler is located in this piece. The input coupler is rigidly attached to a rod linked to a micrometer so as to adjust its penetration into the cavity.
- A flat sample piece, which is the part to be studied, is separated from the cavity body with a vacuum gap of ~ 2.5 mm. An RF probe can be inserted in the gap to provide transmission measurements.

Simulations show that 37% of the RF-induced heating will occur on the sample plate, the remainder being on the cavity (assuming identical materials). The peak magnetic field is located on the sample plate and thus the maximum measurable breakdown field exceeds that of bulk niobium.

The resonator is supported in a cradle placed in a vacuum volume as shown in Figure 7. The cradle is designed so that the two parts of the resonator are thermally isolated from one another. The cavity is mounted onto a support plate strongly connected to the helium tank, while the sample is mounted onto a separate plate supported by a much weaker thermal link. This allows direct measurement of RF losses in the sample using the calorimetric technique described above.

The sample can be changed easily by removing the sample holder and swapping it with another, mounted with a new sample to study. All that needs to be done is to reattach three supporting double-nuts and reconnect the heater and thermometry cables before the vacuum chamber shield can be sealed again.

14

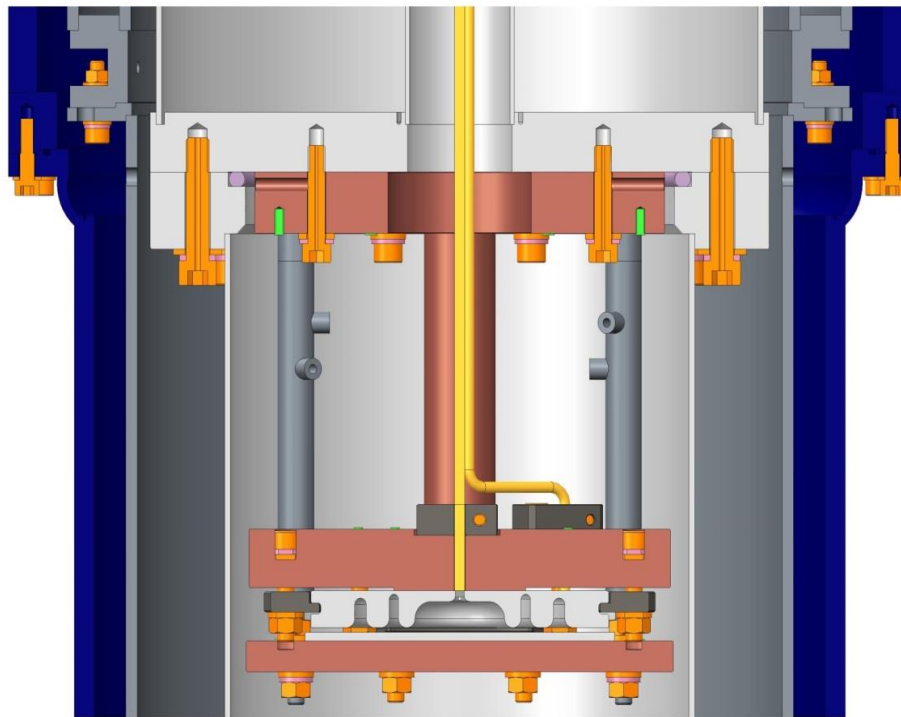


Figure 7: Choked resonator in its cradle (in this case, a 2-choked prototype is depicted). The cavity is connected to the helium bath by a solid copper pillar which provides a strong thermal link to the LHe bath. The sample plate is mounted on a copper plate supported by thin-walled stainless steel pillars which provide a weak thermal link to the LHe bath. The cradle sits in the inner vacuum chamber which is separate from the outer vacuum chamber which provides thermal insulation.

The current choked resonator is a 7.8 GHz design, due to the maximum size of the samples that can be deposited using the equipment available at Daresbury. This allows the testing of sample pieces from 5 cm to 10 cm diameter. The concept can easily be scaled to other frequencies, given a large enough vacuum vessel.

A full cryogenic test hasn't been carried out at time of writing, but is expected to validate the design soon.

4. Summary

In this article we have reviewed devices to characterize SRF materials. These systems have basically two advantages compared to cavity tests. The first one is that small flat samples can be tested. This allowed for example to obtain the surface resistance of MgB_2 with the SIC and of a multilayered sample using the $\text{TE}_{011}/\text{TE}_{012}$ cavity. Neither material is yet sufficiently technologically advanced to be deposited on the inner surface of a cavity. The other advantage is that with a sample test cavity one is not constrained by the field geometry required in an accelerating cavity. This is used in the Quadrupole Resonators with its several resonant modes at different frequencies and almost identical field magnetic configuration. Such a device is therefore ideally suited to test theoretical surface resistance models.

In general the goal for the design of a test cavity is to have a low resonance frequency f_0 , a high magnetic field B_{\max} on the sample, a high ratio of sample to cavity magnetic field $B_{\max \text{ sample}}/B_{\max \text{ cavity}}$ and a high sensitivity. Rate of sample throughput is also important, given the number of samples to test that any optimization process generates. This poses challenging and conflicting design constraints. Some devices currently in use or under development are compared to each other with respect to these parameters in Table 1. Using the Quadrupole Resonators from CERN or HZB it is possible to obtain R_s at multiple frequencies of interest concerning accelerator application over a temperature range inaccessible to standard cavity measurements. The disadvantage of this device is its more complicated sample changing procedure, requiring electron beam welding of a flat sample disk to the sample cylinder. The SIC system is capable of measuring flat samples with high resolution but at higher frequency and lower magnetic field. The Quadrupole Resonators, SIC, Orsay cavity and the Choked Cavity rely on the calorimetric technique to achieve their high resolution. The drawback of this approach is again the more complicated design, since it requires the thermal decoupling of the sample from the host cavity. The Cornell mushroom cavity relying on T-mapping can give a good resolution with a less complicated design. It is however more difficult to derive the absolute value of the surface resistance by this approach. An unmatched maximum field on the sample surface is obtained by the SLAC mushroom cavity. Being made of copper this device has a poor sensitivity making it a more suitable tool for critical field measurements. In summary all devices reviewed in the article can give valuable insights into loss mechanisms under RF and allow the testing of new materials for SRF applications. Each of them has unique features, advantages and disadvantages compared to the others depending on application.

Table 1: Comparison of the different devices and alternative devices.

Device	Frequency [GHz]	Sample diameter [mm]	Sensitivity	B_{\max} [mT]	$B_{\max \text{ sample}}/B_{\max \text{ cavity}}$
SIC	7.4	50	Sub $n\Omega$	14	1.04
Quadrupole Resonator (CERN)	0.4/0.8/1.2	75	Sub $n\Omega$	70	1.18
Quadrupole Resonator (HZB)	0.433/0.866/1.3	75	Sub $n\Omega$	120	0.89
Orsay	4/5.6	126	Few $n\Omega$	16	
SLAC mushroom	11.4	50	0.1 $m\Omega$ Cu cavity /10 $\mu\Omega$ Nb cavity	400	2.5
Cornell mushroom	4.78/6.16	100		106	1.24/1.57
TAMU sapphire-loaded	2.2	178			9.02
Choked resonator	7.8	100	Few $n\Omega$ (est.)	10 (@4.2K)	1.18

5. Outlook

The future of SRF cavity development most likely resides in coatings to improve on cavity properties. A substantial research effort is taking place in that field. However, in order to validate coating methods and

1
2
3
4 479 inform their optimization there is a need for a reliable, affordable and informative method of testing the
5 480 SRF properties of thin film materials. Alternative methods to cavity measurements exist, but they can only
6 481 reveal part of the picture. It is therefore essential to be able to perform measurements of samples in SRF
7 482 conditions.

8 483 The ideal sample test cavity would have a high resolution only obtainable by the calorimetric approach,
9 484 could accommodate small samples of about 2 cm diameter, have a resonance frequency below 3 GHz and
10 485 a maximum field close to the superheating field of niobium. A small sample size is a key aspect to provide
11 486 convenient portability between the RF system, the deposition system and surface analysis tools. Experience
12 487 has shown that a high turnaround not only requires a fairly simple design but also dedicated staff and test
13 488 environment. The cavities that have been developed so far each offer only a partial solution to that need.
14 489 Quadrupole resonators, for instance, provide extremely high-sensitivity measurements over a wide param-
15 490 eter range, but are rather time-consuming to reset for a new sample. This type of instrument is suitable for
16 491 experiments aimed at increasing the understanding of the behavior of thin films on a fundamental level but
17 492 far less suited to sample swapping repeatedly.

20 493 It is however apparent from the backlog of untested samples developed by various teams across the com-
21 494 munity that a cavity that can be used with a fast turn-around time is essential to allow the sorting of prom-
22 495 ising samples from less performing ones. The choked resonator when successfully commissioned could
23 496 fulfill the need for fast turnaround and high precision but still has the drawback of a relatively large sam-
24 497 ple size and high resonant frequency. Further developments should aim to overcome these limitations.
25 498 This cavity would also ideally allow operation at high fields and be a dedicated system with sufficient re-
26 499 source to keep the sample testing rate optimal. Should compromises need to be made, it would be advisa-
27 500 ble to aim for high turnover and medium precision.
28 501
29 502

30 502 31 503 **Acknowledgment**

32 503
33 504
34 505 This work is supported by Jefferson Science Associates, LLC under U.S. DOE Contract No. DE-AC05-
35 506 06OR23177, by DOE under Contract No. DE-SC0004410, by Brookhaven Science Associates, LLC un-
36 507 der US DOE contract No. DE-AC02-98CH10886, and by a Marie Curie International Outgoing Fellow-
37 508 ship within the EU Seventh Framework Programme for Research and Technological Development (2007-
38 509 2013). One of us (TJ) is indebted to the German Ministry of Education and Research for being awarded a
39 510 grant by the German Doctoral Program at CERN (Gentner - Program). This work was also supported by
40 511 the UK Science & Technology Facility Council (STFC). The authors would like to thank Lewis Gurrán
41 512 for his insights into the manuscript.
42 513
43 514

44 514 45 515 **References**

- 46 515
47 516 [1] Poole C P, Farach H A and Creswick R J 1999 Handbook of Superconductivity. (London: Academic
48 517 Press)
- 49 518 [2] Benvenuti C, Circelli N and Hauer M 1984 Niobium Films for Superconducting Accelerating
50 519 Cavities *Appl. Phys. Lett.* **45** 583-4
- 51 520 [3] Padamsee H, Knobloch J and Hays T 1998 *RF Superconductivity for Accelerators* (Weinheim,
52 521 Germany: Wiley-VCH)
- 53 522 [4] Geng R L, Ereemeev G V, Padamsee H and Shemelin V D 2007 High Gradient Studies for ILC With
54 523 Single-Cell Re-Entrant Shape and Elliptical Shape Cavities Made of Fine-Grain and Large-Grain
55 524 Niobium. In: *Proceedings of the 2007 Particle Accelerator Conference*, (Albuquerque, New Mexico)
56 525 p 2337
57
58
59
60

17

- 1
2
3
4 526 [5] Palmieri V 2001 New Materials for Superconducting Radiofrequency Cavities. In: *Proceedings of the 10th Workshop on RF Superconductivity*, (Tsukuba, Japan) p 162
- 5 527
6 528 [6] Posen S, Liepe M and Hall D L 2015 Proof-of-principle demonstration of Nb₃Sn superconducting
7 529 radiofrequency cavities for high Q₀ applications *Appl. Phys. Lett.* **106** 082601
- 8 530 [7] Posen S, Valles N and Liepe M 2015 Radio Frequency Magnetic Field Limits of Nb and Nb₃Sn
9 531 *Physical Review Letters* **115** 047001
- 10 532 [8] Gurevich A 2006 Enhancement of RF Breakdown Field of Superconductors by Multilayer Coating
11 533 *Appl. Phys. Lett.* **88** 012511
- 12 534 [9] James C, Krishnan M, Bures B, Tajima T, Civale L, Edwards R, Spradlin J and Inoue H 2013
13 535 Superconducting Nb Thin Films on Cu for Applications in SRF Accelerators *IEEE*
14 536 *TRANSACTIONS ON APPLIED SUPERCONDUCTIVITY* **23** 3500205
- 15 537 [10] Leviev G I, Genkin V M, Tsindlekht M I, Felner I, Paderno Y B and Filippov V B 2005 Low-
16 538 Frequency Response in the Surface Superconducting State of Single-Crystal ZrB₁₂ *Phys. Rev. B* **71**
17 539 064506
- 18 540 [11] Bahte M, Herrmann F and Schmäser P 1997 Magnetization and Susceptibility Measurements on
19 541 Niobium Samples for Cavity Production. In: *Proceedings of the 1997 Workshop on RF*
20 542 *Superconductivity*, (Abano Terme, Padova, Italy) p 881
- 21 543 [12] Malyshev O B, Gurran L, Pattalwar S, Pattalwar N, Dumbell K D, Valizadeh R and Gurevich A
22 544 2015 A Facility for Magnetic Field Penetration Measurements on Multilayer S-I-S Structures. In:
23 545 *Proceedings of the 17th International Conference on RF Superconductivity*, (Whistler, Canada) p
24 546 716
- 25 547 [13] Antoine C 2012 Materials and surface aspects in the development of SRF Niobium cavities
26 548 *EuCARD Work Package 10: SC RF technology for higher intensity proton accelerators and higher*
27 549 *energy electron linacs, Editorial Series on Accelerator Science*
- 28 550 [14] Ciovati G, Anlage S M, Baldwin C, Cheng G, Flood R, Jordan K, Kneisel P, Morrone M, Nemes G,
29 551 Turlington L, Wang H, Wilson K and Zhang S 2012 Low Temperature Laser Scanning Microscopy
30 552 of a Superconducting Radio-Frequency Cavity *Review of Scientific Instruments* **83** 034704
- 31 553 [15] Gurevich A and Ciovati G 2013 Effect of Vortex Hotspots on the Radio-Frequency Surface
32 554 Resistance of Superconductors *Phys. Rev. B* **87** 054502
- 33 555 [16] Badan L, Durand C, Palmieri V, Preciso R, Stark S, Stivanello F and Venturini W 1998 RF
34 556 Characterization of Small Scale Cavities *Particle Accelerators* **62** 117-23
- 35 557 [17] Palmieri V, Antonio Alessandro R, Sergey Yu S and Ruggero V 2014 Evidence for Thermal
36 558 Boundary Resistance Effects on Superconducting Radiofrequency Cavity Performances *Supercond.*
37 559 *Sci. Technol.* **27** 085004
- 38 560 [18] Yao Z 2015 Medium Field Q-Slope in Low β Resonators. In: *Proceedings of the 17th International*
39 561 *Conference on RF Superconductivity*, (Whistler, Canada)
- 40 562 [19] Tai T, Ghamsari B G, Bieler T R, Tan T, Xi X X and Anlage S M 2014 Near-Field Microwave
41 563 Magnetic Nanoscopy of Superconducting Radio Frequency Cavity Materials *Appl. Phys. Lett.* **104**
42 564 232603
- 43 565 [20] Delayen J R, Bohn C L and Roche C T 1990 Measurements of the Surface Resistance of High-T_c
44 566 Superconductors at High RF Fields *Journal of Superconductivity* **3** 243-50
- 45 567 [21] Allen L H 1986 The Surface Resistance of Superconducting A15 Niobium-Tin Films at 8.6 GHz.
46 568 In: *Department of Physics*, (Standord, California: Stanford University)
- 47 569 [22] Fouaidy M, Bosland P, Ribeauudeau M, Chel S and Juillard M 2002 New Results on RF Properties
48 570 of Superconducting Niobium Films Using a Thermometric System. In: *Proceedings of the 8th*
49 571 *European Particle Accelerator Conference*, (Paris, France: EPS-IGA and CERN) pp 2229-31
- 50
51
52
53
54
55
56
57
58
59
60

- 1
2
3
4 572 [23] Tonkin B A and Proykova Y G 1993 Modular System for Microwave Surface Impedance
5 573 Measurement of High Temperature Superconductors *Supercond. Sci. Technol.* **6** 7
- 6 574 [24] Liang C 1993 A New Surface Resistance Measurement Method with Ultrahigh Sensitivity. In:
7 575 *Physics*, (Blacksburg, Virginia: Virginia Polytechnic Institute and State University)
- 8 576 [25] Kneisel P, Muller G and Reece C 1987 Investigation of the Surface Resistance of Superconducting
9 577 Niobium Using Thermometry in Superfluid Helium *IEEE Transactions on Magnetics* **MAG-23**
10 578 1417-21
- 11 579 [26] Nantista C, Tantawi S, Weisend J, Siemann R, Dolgashev V and Campisi I 2005 Test Bed for
12 580 Superconducting Materials. In: *Proceedings of the 2005 Particle Accelerator Conference*,
13 581 (Knoxville, TN) pp 4227-9
- 14 582 [27] Guo J, Tantawi S, Martin D and Yoneda C 2011 Cryogenic RF Material Testing with a High-Q
15 583 Copper Cavity. In: *Advanced Accelerator Concepts: 14th Workshop*, ed S H Gold and G S
16 584 Nusinovich p 330
- 17 585 [28] Klein N, Muller G, Piel H, Roas B, Schultz L, Klein U and Peiniger M 1988 Millimeter Wave
18 586 Surface Resistance of Epitaxially Grown $\text{YBa}_2\text{Cu}_3\text{O}_{7-x}$ Thin Films *Applied Physics Letter* **54** 3
- 19 587 [29] Misra M, Kataria N D and Srivastava G P 2000 Laterally Resolved Microwave Surface-Resistance
20 588 Measurement of High- T_c Superconductor Samples by Cavity Substitution Technique *IEEE*
21 589 *Transactions on Microwave Theory and Techniques* **48** 791-801
- 22 590 [30] Martinet G, Blivet S, Hammoudi N and Fouaidy M 2009 Development of a TE_{011} Cavity for Thin-
23 591 Films Study. In: *Proceedings of the 14th International Conference on RF Superconductivity*,
24 592 (Berlin-Dresden, Germany) pp 293-6
- 25 593 [31] Phillips L, Davis G K, Delayen J R, Ozelis J P, Plawski T, Wang H and Wu G 2005 A Sapphire
26 594 Loaded TE_{011} Cavity for Superconducting Impedance Measurements - Design, Construction and
27 595 Commissioning Status. In: *Proceedings of the 12th International Workshop on RF*
28 596 *Superconductivity*, (Ithaca, NY) pp 349-51
- 29 597 [32] Xiao B P, Reece C E, Phillips H L, Geng R L, Wang H, Marhauser F and Kelley M J 2011 Radio
30 598 Frequency Surface Impedance Characterization System for Superconducting Samples at 7.5 GHz
31 599 *Review of Scientific Instruments* **82** 056104
- 32 600 [33] Xiao B P 2012 Surface Impedance of Superconducting Radio Frequency Materials. In: *Department*
33 601 *of Applied Science: The College of William and Mary*
- 34 602 [34] Xiao B P, Reece C E, Phillips H L and Kelley M J 2012 Calorimeters for Precision Power
35 603 Dissipation Measurements on Controlled-Temperature Superconducting Radiofrequency Samples
36 604 *Review of Scientific Instruments* **83** 124905
- 37 605 [35] Mahner E, Calatroni S, Chiaveri E, Haebel E and Tessier J M 2003 A New Instrument to Measure
38 606 the Surface Resistance of Superconducting Samples at 400 MHz *Review of Scientific Instruments*
39 607 **74** 3390-4
- 40 608 [36] Junginger T, Weingarten W and Welsch C 2009 RF Characterization of Superconducting Sample.
41 609 In: *Proceedings of the 14th International Conference on RF Superconductivity*, (Berlin-Dresden,
42 610 Germany) pp 130-6
- 43 611 [37] Rubin D L, Green K, Gruschus J, Kirchgessner J, Moffat D, Padamsee H, Sears J, Shu Q S,
44 612 Schneemeyer L F and Waszczak J V 1988 Observation of a Narrow Superconducting Transition at
45 613 6GHz in Crystals of YBCO *Phys. Rev. B* **38** 6538-42
- 46 614 [38] Ormeno R J, Morgan D C, Broun D M, Lee S F and Waldram J R 1997 Sapphire Resonator for the
47 615 Measurement of Surface Impedance of High-Temperature Superconducting Thin Films *Review of*
48 616 *Scientific Instruments* **68** 2121-6
- 49
50
51
52
53
54
55
56
57
58
59
60

19

- 1
2
3
4 617 [39] Bruynseraede Y, Gorle D, Leroy D and Morignot P 1971 Surface-Resistance Measurements in
5 618 TE₀₁₁-Mode Cavities of Superconducting Indium, Lead and an Indium-Lead Alloy at Low and High
6 619 RF Magnetic Fields *Physica* **54** 137-59
- 7 620 [40] Junginger T 2012 Investigations of the Surface Resistance of Superconducting Materials. In:
8 621 *Combined Faculties for the Natural Sciences and for Mathematics*, (Heidelberg, Germany: Ruperto-
9 622 Carola University)
- 10 623 [41] Xie Y 2013 Development of Superconducting RF Sample Host Cavities and Study of Pit-Induced
11 624 Cavity Quench. In: *Department of Physics*, (Ithaca, NY: Cornell University)
- 12 625 [42] Comeaux J K 2014 Testing and Simulation of the SRF Wafer Test Cavity for the Characterization
13 626 of Superconductors and Heterostructures. In: *Department of Physics and Astronomy*, (College
14 627 Station, Texas: Texas A&M University)
- 15 628 [43] Kleindienst R, Burrill A, Keckert S, Knobloch J and Kugeler O 2015 Commissioning Results of the
16 629 HZB Quadrupole Resonator. In: *Proceedings of the 17th International Conference on RF*
17 630 *Superconductivity*, (Whistler, Canada) p 930
- 20 631 [44] Maniscalco J T, Clasby B, Gruber T, Hall D L and Liepe M 2015 Recent Results from the Cornell
21 632 Sample Host Cavity. In: *Proceedings of the 17th International Conference on RF Superconductivity*,
22 633 (Whistler, Canada) p 626
- 23 634 [45] Dhakal P, Ciovati G and Myneni G R 2012 A Path to Higher Q₀ with large grain Niobium cavities.
24 635 In: *International Particle Accelerator Conference 2012*, (New Orleans, Louisiana, USA)
- 25 636 [46] Dhakal P, Ciovati G, Myneni G R, Gray K E, Groll N, Maheshwari P, McRae D M, Pike R, Proslie
26 637 T, Stevie F, Walsh R P, Yang Q and Zasadzinski J 2013 Effect of High Temperature Heat
27 638 Treatments on the Quality Factor of a Large-Grain Superconducting Radio-Frequency Niobium
28 639 Cavity *Phys. Rev. Spec. Top. Accel Beams* **16** 042001
- 30 640 [47] Grassellino A, Romanenko A, Sergatskov D, Melnychuk O, Trenikhina Y, Crawford A, Rowe A,
31 641 Wong M, Khabiboulline T and Barkov F 2013 Nitrogen and Argon Doping of Niobium for
32 642 Superconducting Radio Frequency Cavities: A Pathway to Highly Efficient Accelerating Structures
33 643 *Supercond. Sci. Technol.* **26** 102001
- 34 644 [48] Xiao B P, Geng R L, Kelley M J, Marhauser F, Phillips H L, Reece C E and Wang H 2009 RF
35 645 Surface Impedance Measurement of Polycrystalline and Large Grain Nb Disk Sample at 7.5 GHz.
36 646 In: *Proceedings of the 14th International Conference on RF Superconductivity*, (Berlin-Dresden,
37 647 Germany) p 305
- 40 648 [49] Xiao B P, Geng R L, Kelley M J, Marhauser F, Phillips H L, Reece C E and Wang H 2009
41 649 Commissioning of the SRF Surface Impedance Characterization System at Jefferson Lab. In:
42 650 *Proceedings of the 23rd Particle Accelerator Conference*, (Vancouver, Canada) p 2144
- 43 651 [50] Xiao B P, Zhao X, Spradlin J, Reece C E, Kelley M J, Tan T and Xi X X 2012 Surface Impedance
44 652 Measurements of Single Crystal MgB₂ Films for Radiofrequency Superconductivity Applications
45 653 *Supercond. Sci. Technol.* **25** 095006
- 47 654 [51] Xiao B P, Ereemeev G V, Kelley M J, Phillips H L and Reece C E 2012 RF Surface Impedance
48 655 Characterization of Potential New Materials for SRF-Based Accelerators. In: *Proceedings of XXVI*
49 656 *Linear Accelerator Conference*, (Tel Aviv, Israel) p 312
- 51 657 [52] Lukaszew R A, Beringer D B, Roach W M, Ereemeev G V, Reece C E, Valente-Feliciano A-M and
52 658 Xi X 2013 Proof of Concept Thin Films and Multilayers toward Enhanced Field Gradients in SRF
53 659 Cavities. In: *Proceedings of 16th International Conference on RF Superconductivity*, (Cite
54 660 Internationale Universitaire, Paris, France) p 782
- 55 661 [53] Ereemeev G, Phillips L, Reece C E, Valente-Feliciano A-M and Xiao B P 2013 Characterization of
56 662 Superconducting Samples with SIC System for Thin Film Developments: Status and Recent Results.
- 58
59
60

20

- 1
2
3
4 663 In: *Proceedings of 16th International Conference on RF Superconductivity*, (Cite Internationale
5 664 Universitaire, Paris, France) p 599
- 6 665 [54] Sosa-Guitron S, Gurevich A, Delayen J R, Ereemeev G, Sundhal C and C.-B.Eom 2015
7 666 Measurements of RF Properties of Thin Film Nb₃Sn Superconducting Multilayers using a
8 667 Calorimetric Technique. In: *Proceedings of the 17th International Conference on RF*
9 668 *Superconductivity*, (Whistler, Canada) p 720
- 10 669 [55] Junginger T, Weingarten W and Welsch C 2012 Extension of the Measurement Capabilities of the
11 670 Quadrupole Resonator *Review of Scientific Instruments* **83** 063902
- 12 671 [56] Aull S, Junginger T, Sublet A, Delsolaro W V, Zhang P, Valente-Feliciano A-M and Knobloch J
13 672 2015 On the Understanding of Q-Slope of Niobium Thin Films. In: *Proceedings of the 17th*
14 673 *International Conference on RF Superconductivity*, (Whistler, Canada) p 494
- 15 674 [57] Kleindienst R, Kugeler O and Knobloch J 2013 Development of an Optimized Quadrupole
16 675 Resonator at HZB. In: *Proceedings of 16th International Conference on RF Superconductivity*, (Cite
17 676 Internationale Universitaire, Paris, France) p 614
- 18 677 [58] Keckert S, Kleindienst R, Knobloch J and Kugeler O 2015 Design and First Measurements of an
19 678 Alternative Calorimetry Chamber for the HZB Quadrupole Resonator. In: *Proceedings of the 17th*
20 679 *International Conference on RF Superconductivity*, (Whistler, Canada) p 739
- 21 680 [59] Welander P, Tantawi S and Franzi M 2016 A Test Cavity & Cryostat for Rapid RF Characterization
22 681 of Superconducting Materials. In: *7th International Workshop on Thin Films and New Ideas for*
23 682 *Pushing the Limits of RF Superconductivity*, (Jefferson Lab, Virginia, USA)
- 24 683 [60] Maniscalco J T, Hall D L, Liepe M, Malyshev O B, Valizadeh R and Wilde S 2016 New Material
25 684 Studies in the Cornell Sample Host Cavity. In: *Proceedings of the 7th International Particle*
26 685 *Accelerator Conference*, (BEXCO, Busan Korea)
- 27 686 [61] Pogue N J, McIntyre P M, Sattarov A I and Reece C 2011 Ultra-Gradient Test Cavity for Testing
28 687 SRF Wafer Samples *IEEE TRANSACTIONS ON APPLIED SUPERCONDUCTIVITY* **21** 1903-7
- 29 688 [62] Ribeauveau M, Charrier J P, Chel S, Juillard M, Fouaidy M and Caruette M 1998 RF Surface
30 689 Resistance Measurements of Superconducting Samples with Vacuum Insulated Thermometers. In:
31 690 *Proceedings of the 6th European Particle Accelerator Conference*, (Stockholm, Sweden)
- 32 691 [63] Antoine C Z, Villegier J-C and Martinet G 2013 Study of Nanometric Superconducting Multilayers
33 692 for RF Field Screening Applications *Appl. Phys. Lett.* **102** 102603
- 34 693
35 694
36
37
38
39
40
41
42
43
44
45
46
47
48
49
50
51
52
53
54
55
56
57
58
59
60